PHYSICAL REVIEW A **89**, 033624 (2014)

Impact of scalar potentials on cold atoms with spin-orbit coupling

Fei-Jie Huang, Qi-Hui Chen, and Wu-Ming Liu
National Laboratory for Condensed Matter Physics, Institute of Physics, Chinese Academy of Sciences, Beijing 100190, China
(Received 22 August 2012; published 17 March 2014)

When a gauge potential is constructed from the Berry phase, there is an associated scalar potential coming with the gauge potential. In this paper, we investigate the impact of this scalar potential on cold atoms by constructing an artificial gauge potential in a cold-atomic system. We interpret the scalar potential as the coupling between the atom and the mass of the non-Abelian part of the gauge potential. We demonstrate that the gauge potential can produce spin-orbit coupling and that the scalar potential will suppress the spin Hall currents which are generated by spin-orbit coupling. We also discuss the observation of these phenomena in a real experiment.

DOI: 10.1103/PhysRevA.89.033624 PACS number(s): 67.85.De, 03.65.Vf, 03.75.Ss, 67.85.Lm

I. INTRODUCTION

Spin-orbit (SO) coupling, which is the interaction between the spin and momentum of a particle, is related to many effects in condensed matter physics; especially it is essential for the spin Hall effect [1,2] and topological insulators [3,4]. Recently, with the realization of various artificial gauge potentials, the cold-atom systems also can be designed to simulate SO coupling [5–8]. This opens a new arena to explore novel effects in cold atoms [9–27]. The key to simulating SO coupling is the synthesis of non-Abelian gauge potentials by engineering the interactions between atoms and lasers [8]. Non-Abelian gauge potentials are known to play a crucial role in understanding fundamental interactions in particle physics. In condensed matter physics, non-Abelian gauge potentials also appear in studies on the mechanism of high-T_c superconductivity [28] and graphene [29]. There is no doubt that, to achieve SO coupling with spin $1/2$ in cold atoms, the minimal symmetry of the gauge potentials is required to be SU(2).

The interactions between atoms and lasers can be viewed as an adiabatic approximation of the system, and then the Berry phase exists, these are the reasons why engineering the interactions between atoms and lasers can produce non-Abelian gauge potential. However, in the process of emerging gauge potential, a scalar potential also emerges. This scalar potential cannot be removed, because it originates from the process of constructing the gauge potential. In the current research, one often only pays attention to the investigation of the gauge potential, while ignoring the impact of the scalar potential on the system. In fact, as this paper is to reveal, the scalar potential also has a remarkable effect on the system; therefore, it is also worth investigating the scalar potential. This investigation will give us a better understanding of SO coupling systems which are produced by the artificial non-Abelian gauge potential.

The paper is organized as follows. In Sec. II, we synthesize a SU(2) gauge potential in cold atoms. In the process of synthesize of the gauge potential, a scalar potential will emerge. In Sec. III, we redefine the SU(2) gauge potential, and by reducing the redefined SU(2) gauge potential to the $U(1)$ potential, we interpret the scalar potential as a coupling between the atom and the mass of the non-Abelian part of the gauge potential. In Sec. IV, we show that the SU(2) gauge potential can produce SO coupling, and the scalar potential will suppress the spin Hall currents which are generated by spin-orbit coupling. We discuss how to observe these phenomena in a real experiment by detecting spin Hall currents in Sec. IV. Finally, a brief conclusion is given in Sec. VI.

II. SCALAR POTENTIAL ASSOCIATED WITH GAUGE POTENTIAL IN COLD ATOMS

We consider a cold-atom system with each atom having a three-level Λ-type configuration, as shown in Fig. 1. Two ground states $|g_1\rangle$ and $|g_2\rangle$ are coupled with an excited state $|e\rangle$ through laser fields. The Rabi frequencies are taken as $\Omega_1 = \frac{\Omega}{2}[\exp(i\mathbf{k}\cdot\mathbf{r}) + \exp(i\mathbf{k}'\cdot\mathbf{r})]$ and $\Omega_2 = \frac{\Omega}{2i}[\exp(i\mathbf{k}\cdot\mathbf{r}) - \exp(i\mathbf{k}'\cdot\mathbf{r})]$, in which $\mathbf{k}$ and $\mathbf{k}'$ are the wave vectors of lasers, $\mathbf{k}' = e^{i\varphi}\mathbf{k}$, $\mathbf{r}$ is the position vector, and φ is the angle between the lasers as shown in Fig. 1(b). The total Rabi frequency is given by $\Omega = (|\Omega_1|^2 + |\Omega_2|^2)^{1/2}$. The Hamiltonian reads $H = H_k + H_I$, in which $H_k = p^2/2m$ is the kinetic energy of a single cold atom, p is the momentum, and m is the atomic mass. The interacting Hamiltonian is given by $H_I = 2\Delta|e\rangle\langle e| + (\Omega_1|e\rangle\langle g_1| + \Omega_2|e\rangle\langle g_2| + \text{H.c.})$, where Δ is the detuning.

By defining $\mathbf{Q} = \mathbf{k} + \mathbf{k}'$ as the total wave vector of laser fields and $\mathbf{q} = \mathbf{k} - \mathbf{k}'$ as the relative wave vector, the eigenvectors of interacting Hamiltonian can be expressed as

$$\begin{aligned}
|\chi_{D1}\rangle &= -\sin\theta|g_1\rangle + \cos\theta|g_2\rangle,\\
|\chi_{D2}\rangle &= -\exp(i\phi)\sin\delta|e\rangle + \cos\delta\cos\theta|g_1\rangle\\
&\quad + \cos\delta\sin\theta|g_2\rangle,\\
|\chi_3\rangle &= \exp(i\phi)\cos\delta|e\rangle + \sin\delta\cos\theta|g_1\rangle\\
&\quad + \sin\delta\sin\theta|g_2\rangle,
\end{aligned} \tag{1}$$

with eigenvalues of 0, $\frac{\Omega}{2\Delta}$, and 2Δ, respectively, in which $\delta = \arctan[(\frac{\Delta^2}{\Omega^2} + 1)^{1/2} - \frac{\Delta}{\Omega}]$, $\phi = \frac{1}{2}\mathbf{Q}\cdot\mathbf{r}$, $\theta = \frac{1}{2}\mathbf{q}\cdot\mathbf{r}$.

For large detuning, we can neglect the eigenvalue 2Δ and assume that the other two eigenvalues are degenerate. Hence, by utilizing the Berry phase, the remaining two eigenvectors of the interacting Hamiltonian give rise to an effective SU(2) gauge potential $\mathbf{A}_{\alpha\beta} = -i\langle\chi_\alpha|\nabla|\chi_\beta\rangle$, $\alpha,\beta = D1, D2$, with its explicit expression

$$\mathbf{A} = \tfrac{1}{2}\mathbf{q}\sigma_y + \tfrac{1}{4}\delta^2\mathbf{Q}\sigma_z, \tag{2}$$

where $\sigma_i, i = x,y,z$ are the Pauli matrices. Also, a scalar potential $V_{\alpha\beta} = \frac{1}{2m}\langle\nabla\chi_\alpha|\nabla\chi_\beta\rangle + \frac{1}{2m}|\langle\chi_\alpha|\nabla|\chi_\beta\rangle|^2$ comes with gauge potential $\mathbf{A}$ in the process of constructing $\mathbf{A}$, with its

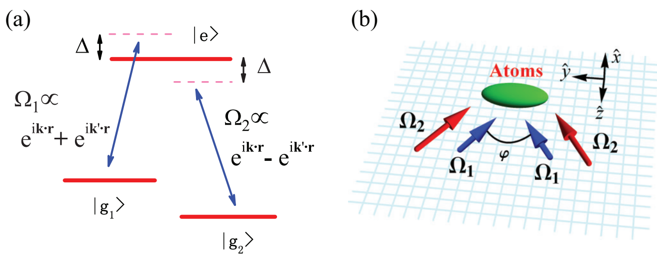

FIG. 1. (Color online) (a) Configuration of three-level Λ-type atoms interacting with laser fields. Two ground states $|g_1\rangle$ and $|g_2\rangle$ are coupled with an excited state $|e\rangle$ through laser fields. Ω_1 and Ω_2 are Rabi frequencies; Δ is a large detuning. (b) Configuration of laser fields. Two inner laser fields (short blue arrows) are arranged to form Rabi frequency Ω_1, and the other two lasers (long red arrows) are arranged to form Ω_2. There is an angle φ between laser fields.

explicit expression

$$\begin{aligned} V &= \left\{ \frac{1}{16m}\delta^2[q^2 - (1+\delta^2)Q^2] + \delta\frac{\Omega}{2} \right\} \sigma_z \\ &= M_0\sigma_z. \end{aligned} \tag{3}$$

III. INTERPRETATION OF SCALAR POTENTIAL

We will give an interpretation of scalar potential V in this section. Because the momentum p is a good quantum number, we discuss the system in the momentum space. First, the gauge potential $\mathbf{A}$ can be redefined as

$$\mathcal{A}_0 = \gamma \cdot \mathbf{A}, \tag{4}$$

where $\gamma = \mathbf{p}/p$ is a dimensionless parameter; then neglecting the constant terms, the effective Hamiltonian reads

$$H = H_k + g\mathcal{A}_0 + V, \tag{5}$$

where $g = p/m$ is a nonrelativistic dimensionless strength factor (assuming that the light velocity $c = 1$).

Denote $\mathbf{n} = (n_x, n_y, n_z)$ as a unit vector of gauge potential $\mathbf{A}$ in SU(2) space, and define the direction vector as $\sigma(t) = \sum_i n_i\sigma_i(t)\hat{i}$, where t is time, $i = x,y,z$. By assuming that $\sigma_i(t)$ depends on time, we now study the system in the Heisenberg representation. The definition implies that we choose the same directions for external and internal spaces at the initial time. Then, along the direction vector σ, $\mathcal{A}_0$ (see Fig. 2), which depends on time in the Heisenberg representation, can be decomposed to two gauge potentials $\mathcal{A}_0 = \mathcal{A} + \mathcal{B}$ [30–32], with

$$\begin{aligned} \mathcal{A} &= (\sigma\cdot\mathcal{A}_0)\sigma + [\partial_0\sigma,\sigma], \\ \mathcal{B} &= [\sigma,\nabla_0\sigma], \end{aligned} \tag{6}$$

where $\nabla_0 = \partial_0 + [\mathcal{A}_0,]$ represents the time component of covariant derivative, and $[,]$ denotes the commutator. According to reduction theorem, when $\mathcal{A}_0$ is reducible to the $U(1)$ potential,

$$\nabla_0\sigma = 0. \tag{7}$$

This condition is actually a parallel transportation. It demonstrates that when $\mathcal{A}_0$ is in parallel transportation, it becomes $U(1)$ gauge potential $\mathcal{A}$.

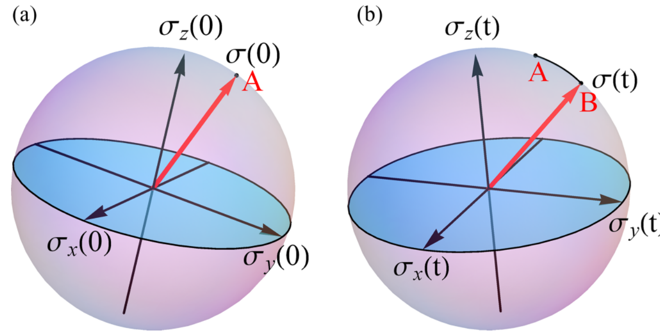

FIG. 2. (Color online) Sphere surface of SU(2) gauge potential $\mathcal{A}_0$. (a) At the initial time $t = 0$, the basic vectors of the gauge potential $\sigma_x(0)$, $\sigma_y(0)$, and $\sigma_z(0)$ point to certain directions. The direction vector (red arrow) $\sigma(0)$ points to A. (b) After time t, the basic vectors change to $\sigma_x(t)$, $\sigma_y(t)$, and $\sigma_z(t)$ directions. The direction vector $\sigma(t)$ changes along with the basic vectors and points to B. If path AB is a parallel transportation, $\mathcal{A}_0$ reduces to an Abelian gauge potential.

We now discuss gauge potential $\mathcal{B}$, which can be viewed as the non-Abelian part of $\mathcal{A}_0$. Taking the Planck constant $\hbar = 1$, then $\partial_0 = i\partial_t$ corresponds to the Hamiltonian operator, and ∂_0 in the $U(1)$ gauge potential $\mathcal{A}$ becomes $i\partial_t\sigma = [\sigma,H]$. This equation is actually the equation of motion of spin. Using Eq. (7), $\nabla_0\sigma$ in the gauge potential $\mathcal{B}$ can be written as

$$\nabla_0\sigma = [\sigma,H] + [\mathcal{A}_0,\sigma] = [\sigma,V], \tag{8}$$

and the gauge potential $\mathcal{B}$ reads

$$\mathcal{B} = [\sigma,[\sigma,V]]. \tag{9}$$

From this equation, it can be learned that the scalar potential V in fact relates to the gauge potential $\mathcal{B}$.

To investigate the scalar potential V further, we discuss the action of gauge potential $\mathcal{A}_0$. Because $\mathcal{A}_0$ has only a time component, we expand the action of this gauge potential as $S = \mathrm{Tr}F_{0i}F_{0i} + \frac{1}{2}\mathrm{Tr}F_{00}F_{00}$, where 0 is the time component and i are space component indices; the gauge strengths read $F_{0i} = -\partial_i\mathcal{A}_0$, $F_{00} = [\mathcal{A}_0,\mathcal{A}_0]$. As the mass term is related to the time component of the action, thus the second term of action S indicates a mass term. When $\mathcal{A}_0$ is substituted to this term, we have $\frac{1}{2}\mathrm{Tr}F_{00}F_{00} = M_B^2\mathrm{Tr}[\mathcal{B}\cdot\mathcal{B}]$, in which M_B is mass. In this case, the action of gauge potential $\mathcal{A}_0$ has the expression $S = S_A + S_B$, with $S_A = \mathrm{Tr}[\nabla\mathcal{A}\cdot\nabla\mathcal{A}]$ presenting the action of the Abelian part of gauge potential $\mathcal{A}_0$, and

$$S_B = \mathrm{Tr}[\nabla\mathcal{B}\cdot\nabla\mathcal{B}] + M_B^2\mathrm{Tr}[\mathcal{B}\cdot\mathcal{B}], \tag{10}$$

with S_B presenting the action of the non-Abelian part of $\mathcal{A}_0$. Comparing S_A and S_B, we find that S_A only has the kinetic term, while S_B not only has a kinetic term, but also a mass term. This is obvious because in general in gauge theories, the Abelian gauge potential does not have self-interaction, whereas the non-Abelian gauge potential has a self-interaction term which plays the role of the mass term.

From the expression of gauge strength F_{00}, the mass M_B in S_B reads

$$M_B = M_0/[1 + (\mathbf{Q}\cdot\mathbf{p}/2\mathbf{q}\cdot\mathbf{p})^2\delta^4]^{\frac{1}{2}}. \tag{11}$$

For $V = M_0\sigma_z$ in Eq. (3), V can be written as

$$V = \eta' M_B \sigma_z, \tag{12}$$

where $\eta' = [1 + (\mathbf{Q}\cdot\mathbf{p}/2\mathbf{q}\cdot\mathbf{p})^2\delta^4]^{\frac{1}{2}}$ is a dimensionless coupling factor. It is clear that from this equation, the scalar potential V in fact describes the coupling between the mass of gauge potential $\mathcal{B}$ and the atom.

Considering gauge potentials $\mathcal{A}$ and $\mathcal{B}$ in $\mathcal{A}_0$, the effective Hamiltonian in Eq. (5) can be written as

$$H = H_k + H_A + H_B, \tag{13}$$

in which $H_A = g\mathcal{A}$ presents the coupling between the Abelian part of gauge potential $\mathcal{A}_0$ and the atom.

$$H_B = g\mathcal{B} + \eta' M_B \sigma_z, \tag{14}$$

in which $g\mathcal{B}$ can be viewed as the coupling between the kinetic term of non-Abelian part of gauge potential $\mathcal{A}_0$ and the atom, and the scalar potential $V = \eta' M_B\sigma_z$, as explaining above, describes the coupling between the mass term and the atom.

IV. IMPACT OF SCALAR POTENTIAL ON COLD ATOMS

Atomic trajectories impacted by scalar potential V can be calculated from the equation of motion $\dot{\mathbf{r}} = -i[\mathbf{r}, H_B]$. As shown in Fig. 3(a), the contribution includes two opposite trajectories. Figure 3(b) shows the dispersion of H_B. The dispersion is linear, and the energy does not vanish at zero momentum due to the presence of mass M_B.

The goal of synthesis of non-Abelian gauge potentials is to simulate SO coupling in cold atoms; thus we investigate the impact of scalar potential on SO coupling. The SO coupling term reads $H_{\text{SO}} = g\mathcal{A}_0$; namely, the whole gauge potential $\mathcal{A}_0$, including Abelian and non-Abelian parts of the gauge potential, participates in SO coupling. With Eq. (2) and Eq. (4), the explicit expression of SO coupling is

$$H_{\text{SO}} = \lambda\sigma_y + \nu\sigma_z. \tag{15}$$

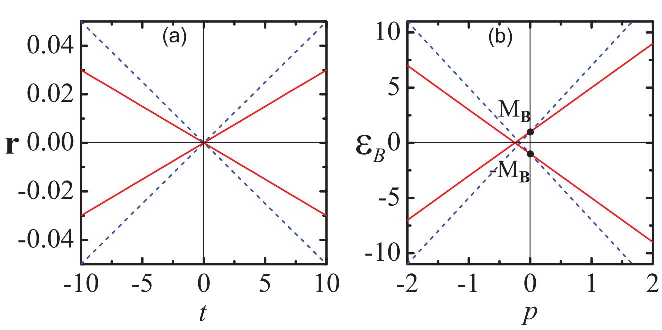

FIG. 3. (Color online) (a) Atomic trajectories impacted by scalar potential V. The red solid and blue dashed lines correspond to the velocities $v = 3\times10^{-3}$ μm/s and $v = 5\times10^{-3}$ μm/s, respectively. $\mathbf{r}$ and t are in units of μm and s. (b) Dispersion of coupling energy between gauge potential $\mathcal{B}$ and a single atom, $\varepsilon_B = \pm(\epsilon p + \eta' M_B)$. The solid red and dashed blue lines correspond to the coupling strength parameters $\epsilon = 4m^{-1}\times10^{-2}$ and $\epsilon = 6m^{-1}\times10^{-2}$, respectively. ε_B and p are in units of recoil energy $\varepsilon_R = k^2/(2m)$ and recoil momentum k.

The coupling strength factors λ and ν are $\lambda = \frac{1}{2m}\mathbf{q}\cdot\mathbf{p}$ and $\nu = \frac{1}{4m}\delta^2\mathbf{Q}\cdot\mathbf{p}$, respectively.

To investigate the impact of scalar potential on SO coupling, a two-dimensional harmonic potential $\frac{1}{2}m\omega^2(y^2+z^2)$ is chosen to trap the cold atoms. The Hamiltonian of the system is as follows. The wave vectors of the lasers are chosen as $k_x = k'_x = 0$, and the internal space is rotated $\pi/2$ around the x direction. Combining Eq. (12) and Eq. (15) yields the explicit expression of the Hamiltonian:

$$H(p,r) = \frac{p^2}{2m} + \frac{\mathbf{Q}\cdot\mathbf{p}}{4m}\delta^2\sigma_y + \frac{\mathbf{q}\cdot\mathbf{p}}{2m}\sigma_z + \eta' M_B\sigma_z + \frac{1}{2}m\omega^2(y^2+z^2). \tag{16}$$

By diagonalizing the Hamiltonian, we obtain

$$H_\pm(p,r) = \frac{p^2}{2m} \pm \left(\frac{\mathbf{q}\cdot\mathbf{p}}{2m} + M_B\right) + \frac{1}{2}m\omega^2 z^2 + \frac{1}{2}m\omega^2\left(1 \pm \frac{2m^*}{M_B}\right)y^2, \tag{17}$$

in which $m^* = q^2/2m$ is a characteristic mass of the system. From $\dot{\mathbf{r}} = -i[\mathbf{r}, H]$, the time-evolved Hamiltonian can be written as

$$H_\pm(p,r,t) = \frac{p^2}{2m} \pm \left(\frac{\mathbf{q}\cdot\mathbf{p}}{2m} + M_B\right) + \frac{1}{2}m\omega^2 z^2 + \frac{1}{2}m\omega^2\left(1 \pm \frac{2m^*}{M_B}\right)\left(y \pm \frac{\mathbf{q}\cdot\mathbf{p}}{2m}t\right)^2. \tag{18}$$

The relationship between the particle number N and trap frequency ω is given by solving the equation

$$N = \int d\mathbf{r}\, n(r, t=0, T=0), \tag{19}$$

in which

$$n(r,t,T) = \frac{1}{(2\pi)^2}\int d\mathbf{p}[f_+(p,r,t,T) + f_-(p,r,t,T)] \tag{20}$$

is the density profile of the cold atoms, $f_{\sigma_z} = f_\pm(p,r,t,T) = [e^{\beta(H_\pm(p,r,t)-\mu)}+1]^{-1}$ are the spin-depending Fermi distributions with $\beta = 1/k_BT$, and k_B and T are the Boltzmann constant and temperature, respectively. The relation is shown in Fig. 4.

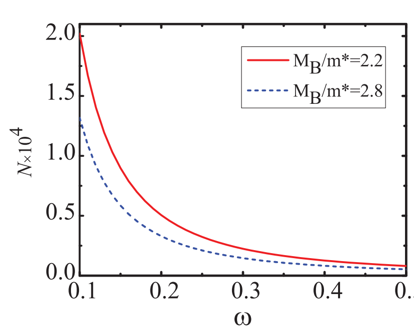

FIG. 4. (Color online) Relation between the particle number N and trap frequency ω. The solid red and dashed blue lines correspond to the ratios $M_B/m^* = 2.2$ and $M_B/m^* = 2.8$, respectively. The unit of ω is taken to be $0.1\varepsilon_F$, where ε_F is Fermi energy.

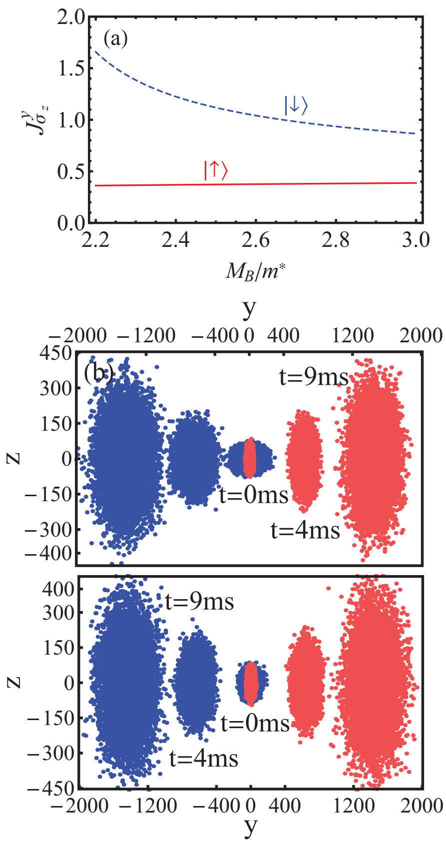

FIG. 5. (Color online) (a) Relation between the mass M_B and the spin Hall currents $J^y_{\sigma_z}$. The solid red (dashed blue) line corresponds to the spin up (down) current. The unit of $J^y_{\sigma_z}$ is $\frac{1}{2\pi}\times 10$ cm/s. (b) Evolution of the atomic density profile from time $t = 0$ ms to $t = 4$ ms and $t = 9$ ms. The red (light gray) and blue (dark gray) parts in each figure denote the spin-up and spin-down atoms. The unit of y and z directions is μm. The temperature is taken as $T = 0.4T_F$, where T_F is Fermi temperature. The up and down figures correspond to the ratios $M_B/m^* = 2.2$ and $M_B/m^* = 2.8$, respectively. The figures show the trends of spin currents of Fig. 5(a).

We now discuss the spin Hall currents of the system. To generate spin Hall currents, the wave vectors of the lasers are chosen as $k_x = k'_x = 0$, and the internal space is rotated $\pi/2$ around the x direction. In this case, the SO coupling reads $H_{\mathrm{SO}} = \lambda\sigma_z$. This term describes the spin Hall currents in which the spin is polarized in the z direction while the currents move along the y direction. The spin Hall currents can be written as

$$J^y_{\sigma_z} = \frac{1}{(2\pi)^2}\int d\mathbf{p}\, f_{\sigma_z}(p)\, j^y_{\sigma_z}, \tag{21}$$

where $j^y_{\sigma_z} = \langle \hat{j}^y_{\sigma_z}\rangle$ are the single-particle currents, $\hat{j}^y_{\sigma_z} = \frac{1}{4}[\sigma_z, v_y]_+$ are the spin current operators, and $v_y = -i[y,H]$ is the velocity along the y direction. The impact of scalar potential V on the spin Hall currents is shown in Fig. 5(a). The spin-down current is suppressed by the increase of the mass M_B, whereas the spin-up current grows slightly. The evolution of the atomic density profile $n(r,t)$ is shown in Fig. 5(b).

V. EXPERIMENTAL SIGNATURES OF IMPACT OF SCALAR POTENTIAL

We now discuss the observation of impact of the scalar potential V by detecting spin Hall currents. We choose ^{6}Li atoms for a three-level Λ-type system, with a particle number of about 10^4, and a $2\pi \times 10^2$ Hz harmonic potential is used to trap the atoms. The configuration of four laser fields is shown in Fig. 1(b). The wave number of the lasers can be taken as $2\pi \times 1.0\ (\mu\mathrm{m})^{-1}$ [7]. For large detuning, Rabi frequency and detuning are required to satisfy $\Omega^2/\Delta \sim 10^6 Hz$. When the laser fields are turned on, the non-Abelian gauge potential is applied to the ^{6}Li atoms. By tuning the angle φ between the lasers, different masses of gauge potential $\mathcal{B}$ can be obtained.

To detect the spin-up current, we first initialize the atoms in the $|g_1\rangle$ ground state. Then a Raman pulse is applied between states $|g_1\rangle$ and $|g_2\rangle$ to transfer the atoms to the spin-up state $|\chi_{D1}\rangle$. The Rabi frequency of the pulse is required to match the spatial variation of $|\chi_{D1}\rangle$. Turning on the lasers, the cold atoms will experience the SO coupling and also the scalar potential V. After time t, we turn off the lasers and apply a reversal Raman pulse to transfer the atoms back to the initial state. Using time-of-flight measurement, the spin-up current of the system can be determined. The measurement of the spin-down current (corresponding to the $|\chi_{D2}\rangle$ state) also can be detected in the same manner [33].

VI. CONCLUSION

In summary, we have investigated the impact of scalar potential V on cold atoms by constructing SO coupling through an artificial non-Abelian gauge potential in a cold-atomic system. We interpret the scalar potential as the coupling between the mass of gauge potential $\mathcal{B}$ and the atom. We demonstrate that the scalar potential V can suppress the spin Hall currents which are generated by spin-orbit coupling. We also discuss the observation of these phenomena in a real experiment. Our results are not only confined to the cold-atomic system that we have discussed, but can also be applied to systems concerning the Berry phase. We expect that the exploration of the impact of the scalar potential V can help to understand the effect of SO coupling in cold atoms.

ACKNOWLEDGMENTS

This work was supported by NKBRSFC under Grants No. 2011CB921502 and No. 2012CB821305, and the NSFC under Grants No. 61227902 and No. 61378017.

[1] S. Murakami, N. Nagaosa, and S. C. Zhang, Science **301**, 1348 (2003).
[2] J. Sinova, D. Culcer, Q. Niu, N. A. Sinitsyn, T. Jungwirth, and A. H. MacDonald, Phys. Rev. Lett. **92**, 126603 (2004).
[3] M. Z. Hasan and C. L. Kane, Rev. Mod. Phys. **82**, 3045 (2010).
[4] X. L. Qi and S. C. Zhang, Rev. Mod. Phys. **83**, 1057 (2011).
[5] Y. J. Lin, K. Jiménez-Garcia, J. V. Prto, and I. B. Spielman, Nature (London) **471**, 83 (2011).

[6] P. Wang, Z. Q. Yu, Z. Fu, J. Miao, L. Huang, S. Chai, H. Zhai, and J. Zhang, Phys. Rev. Lett. **109**, 095301 (2012).
[7] L. W. Cheuk, A. T. Sommer, Z. Hadzibabic, T. Yefsah, W. S. Bakr, and M. W. Zwierlein, Phys. Rev. Lett. **109**, 095302 (2012).
[8] J. Dalibard, F. Gerbier, G. Juzeliūnas, and P. Öhberg, Rev. Mod. Phys. **83**, 1523 (2011).
[9] J. Ruseckas, G. Juzeliunas, P. Öhberg, and M. Fleischhauer, Phys. Rev. Lett. **95**, 010404 (2005).
[10] S. L. Zhu, H. Fu, C. J. Wu, S. C. Zhang, and L. M. Duan, Phys. Rev. Lett. **97**, 240401 (2006).
[11] X. J. Liu, M. F. Borunda, X. Liu, and J. Sinova, Phys. Rev. Lett. **102**, 046402 (2009).
[12] C. Wang, C. Gao, C. M. Jian, and H. Zhai, Phys. Rev. Lett. **105**, 160403 (2010).
[13] M. Iskin and A. L. Subasi, Phys. Rev. Lett. **107**, 050402 (2011).
[14] E. van der Bijl and R. A. Duine, Phys. Rev. Lett. **107**, 195302 (2011).
[15] S. Sinha, R. Nath, and L. Santos, Phys. Rev. Lett. **107**, 270401 (2011).
[16] H. Hu, L. Jiang, X. J. Liu, and H. Pu, Phys. Rev. Lett. **107**, 195304 (2011).
[17] R. Liao, Y. Yi-Xiang, and W. M. Liu, Phys. Rev. Lett. **108**, 080406 (2012).
[18] Y. Deng, J. Cheng, H. Jing, C. P. Sun, and S. Yi, Phys. Rev. Lett. **108**, 125301 (2012).
[19] T. Ozawa and G. Baym, Phys. Rev. Lett. **109**, 025301 (2012).
[20] J. Y. Zhang, S. C. Ji, Z. Chen, L. Zhang, Z. D. Du, B. Yan, G. S. Pan, B. Zhao, Y. J. Deng, H. Zhai, S. Chen, and J. W. Pan, Phys. Rev. Lett. **109**, 115301 (2012).
[21] K. Seo, C. Zhang, and S. Tewari, Phys. Rev. A **88**, 063601 (2013).
[22] C. J. Kennedy, G. A. Siviloglou, H. Miyake, W. C. Burton, and W. Ketterle, Phys. Rev. Lett. **111**, 225301 (2013).
[23] R. Gupta, G. S. Singh, and J. Bosse, Phys. Rev. A **88**, 053607 (2013).
[24] Y. Li, Giovanni I. Martone, L. P. Pitaevskii, and S. Stringari, Phys. Rev. Lett. **110**, 235302 (2013).
[25] T. Zhou and Z. D. Wang, Phys. Rev. B **88**, 155114 (2013).
[26] C. Qu, C. Hamner, M. Gong, C. Zhang, and P. Engels, Phys. Rev. A **88**, 021604 (2013).
[27] J. Larson, B. M. Anderson, and A. Altland, Phys. Rev. A **87**, 013624 (2013).
[28] P. A. Lee, N. Nagaosa, and X. G. Wen, Rev. Mod. Phys. **78**, 17 (2006).
[29] M. A. H. Vozmedianoa, M. I. Katsnelsonb, and F. Guinea, Phys. Rep. **496**, 109 (2010).
[30] Y. M. Cho, Phys. Rev. D **21**, 1080 (1980).
[31] L. Faddeev and A. J. Niemi, Phys. Rev. Lett. **82**, 1624 (1999).
[32] L. Faddeev and A. J. Niemi, Nucl. Phys. B **776**, 38 (2007).
[33] T. D. Stanescu, C. Zhang, and V. Galitski, Phys. Rev. Lett. **99**, 110403 (2007).